Chapter 4
Characterization of PAM/PVA Blends

Abstract

This chapter gives an account of the characteristics of Poly acrylamide(PAM) and Poly vinyl alcohol (PVA) blend in different weight proportion (70/30, 50/50 and 30/70 wt %) which is prepared by solution cast technique. These blends are investigated by spectroscopic techniques like FTIR, UV-Vis and RAMAN. Mechanical, Thermal and Morphological properties are also investigated. The results obtained from different characterization techniques show the effect of blending on different properties. These properties of PAM/PVA blends are correlated with spectroscopic investigation.

4.1. Introduction

In the recent trends, polymer blends cover many different product areas. Their applications in different fields increase drastically. The polymer blends are widely used in biomedical field. The accomplishment of polymer as bio materials depends on their mechanical and thermal properties which allow different shapes with low production cost. Biological polymers have poor mechanical properties. So considering these factors, we prepared polymer blends which have good mechanical, thermal and optical properties with good compatibility.

The selection and use of polymers can potentially form hydrogen bonds when two polymers are mixed, as well as the study of the properties of the blends are of importance to find further applications of the resulting blend materials for biomedical and pharmaceutical devices [1]. PAM is well-known hydrophilic polymer and has been greatly used in the field of agriculture and biomedicine [2, 3]. The electrical and mechanical properties of the ethylene propylene diene monomer (EPDM) and nitrile rubber (NBR) blended with polyacrylamide (PAM) were studied [4]. PAM is a polymer of biomedical and pharmaceutical interest widely studied as hydrogel for blood compatible applications [5]. Polymers of acrylamide are well known for their hydrophilicity and inertness that make them a material of choice in large number of applications in medical and pharmacy [6]. Many researchers have studied the use of PAM hydrogels for controlled release of fertilizers, pesticides or possibly in medicine and also as electrolyte solution [6-8]. Also, it was used for water retention in arid soils [9]. Polyacrylamide-based polymers have received a great extent of utility in industry because of their high molecular weight, water soluble property, and ability to receive diverse modification on chemical structure [10, 11]. When PAM is dissolved in solvents, the linear structure formed in solution. Which reduces the drag coefficient and thereby, facilitating the transportation of these viscous liquids over long distances

[12, 13]. When cross-linked, the polymer is insoluble in water and forms a hydrogel system that is capable of absorbing and retaining large quantities of water. The linear form and solubility properties are also offer unique applications such as stabilizing soil matrices, reducing erosion, and improving soil aeration [9, 14-15].

Poly vinyl alcohol (PVA) films are known to have high tensile and impact strengths, a high tensile modulus, and excellent resistance to alkali, oil, and solvents [16]. PVA has gained increasing attention in the biomedical field because of its bio inertness [17, 18]. Vargas et al. [19] investigated poly Vinyl Alcohol (PVA) for the phase behavior. Fritz and Breitsmer developed ionically conducting polyelectrolytes based on PVA, because of its bio-compatibility and wide use in biomedical fields [20, 21]. Because of its superior mechanical properties and better ionic conduction, it has some technological advantages in electro chromic devices and fuel cells, etc. [22]. Hydrophilic nature of PVA is beneficial for its applications, and also a limiting factor in its characterization because its molecules combine through hydrogen bonding due to its poly hydroxyl groups [23]. The chemical resistance and physical properties of PVA have led to its broad industrial use. Due to its oleophobic nature, PVA is useful as membrane for water waste treatment as well as filtration membrane [24, 25]. Chemically cross linked PVA hydrogels have received increasing attention in biomedical and biochemical applications because of their permeability, biocompatibility and biodegradability [26-28]. Hydrogel blend of Polyacrylamide and Poly Vinyl Alcohol can be used as proton exchange membrane [29]. Blends of polyvinyl alcohol (PVA) with other polymers have been mechanically characterized by many researchers [30-32]. Horia M Nizam El-din et. al. undertaken to investigate the miscibility of PVA with PAM in various proportions [31]. PVA and PAM are two well-known polymers and their individual biomedical, mechanical and other properties have been thoroughly investigated [6, 32-

33]. PVA is a water soluble, non-toxic, non-immunogenic polymer with a remarkable film forming property [34, 35]. However, its weak mechanical strength restricts its use in those applications where the material has to withstand stretched stress. The introduction of other polymeric components into the PVA matrix could improve its mechanical properties [36].

4.2. Results and Discussion

4.2.1. FTIR Analysis

FTIR is very important technique for the study of the molecular interactions. The width and intensity of spectral bands, as well as the position of peaks are all sensitive to environmental changes and to conformations of the macromolecule at molecular level. These differences would be derived from chemical interactions resulting in the band shifts and broadening. If the polymers are compatible, there should be considerable differences between the infrared spectra of the blend and the pure components [37]. So we can study the compatibility as well as intermolecular interactions between two polymers.

Figure 4.1 (a, b) shows FTIR absorption spectra of pure PAM, pure PVA and PAM/PVA blend with different concentrations recorded at room temperature in the region 400 – 4000 cm^{-1}. FTIR absorption bands, positions and its assignments of all prepared composite films are listed in **Table 4.1** [38-40]. De-convolution was made for two spectral regions 1500 – 1800 cm^{-1} and 2600 – 3700 cm^{-1} as shown in **Figure 4.2 (a, b)**. From the deconvolution, the spectral peaks are well separated which are listed in **Table 4.1**.

The IR spectrum of PAM exhibiting bands at 3105 cm^{-1} and 3302 cm^{-1} which were assigned to a symmetric and asymmetric stretching vibration of N–H, bands at 2763 cm^{-1} and 2926 cm^{-1} assigned to –CH symmetric and asymmetric stretching respectively, bands at 1728 cm^{-1} (C=O

stretching) and 1600 cm^{-1} assigned to (N–H bending) [41, 42]. The band at 1652 cm^{-1} corresponds to the asymmetric stretching vibration of $–COO^-$ groups while bands at 1434 cm^{-1} (C–N stretching), 1375 cm^{-1} ($–CH_2$ wagging), 1359 cm^{-1} (C–H bending), 1254 cm^{-1} ($–NH_2$ wagging), 1097 cm^{-1} (C–C stretching) were also detected [38].

For pure PVA, the bands at 3000 cm^{-1} to 3600 cm^{-1} assigned to –OH stretching region and 1565 cm^{-1} assigned to bending vibration of hydroxyl group [42]. The band corresponding to methylene group ($–CH_2$), asymmetric and symmetric stretching vibrations occurs at about 2925 cm^{-1} and 2759 cm^{-1}. The band at about 936 cm^{-1} corresponds to C–O stretching of acetyl groups, present on the PVA backbone [43, 44]. PVA spectrum also exhibited peaks at 1433 cm^{-1}, 1360 cm^{-1}, 1254 cm^{-1},1119 cm^{-1} and 1042 cm^{-1} which assigned as O–H & C–H bending, $–CH_2$ out of plane bending, $–CH_2$ bending, C–O–C asymmetric and symmetric Stretching respectively. A band at 1727 cm^{-1} is corresponding to the C=O group present in PVA [45]. The spectra of the blend films are characterized by the presence of the absorption bands typical of the pure polymer. The peaks appeared in the range 3,000 cm^{-1}–2,800 cm^{-1} indicates the presence of $–CH_2$ groups in all the spectra. Bands of PAM at 3302 cm^{-1} and 3105 cm^{-1} which are stretching vibration of $–NH_2$ group involved in both inter and intra molecular interaction of hydrogen bond coupled with –OH group of PVA at 3145 cm^{-1} and 3305 cm^{-1} when PVA added into PAM polymer matrix. Spectra of blends clearly indicate the increase in the intensity of bands in the region of 3000 cm^{-1} to 3600 cm^{-1}. But intensity of this broad band is maximum for 50/50 blend ratio than the others and peak shifting (at 3149 cm^{-1} and 3342 cm^{-1}) in this region is towards higher wave number side, which indicates the strong hydrogen bonding between PAM and PVA due to $–CONH_2$ groups in PAM and –OH group in PVA, hence this blue shift of IR band indicating enhancement of bond strength [46-48].

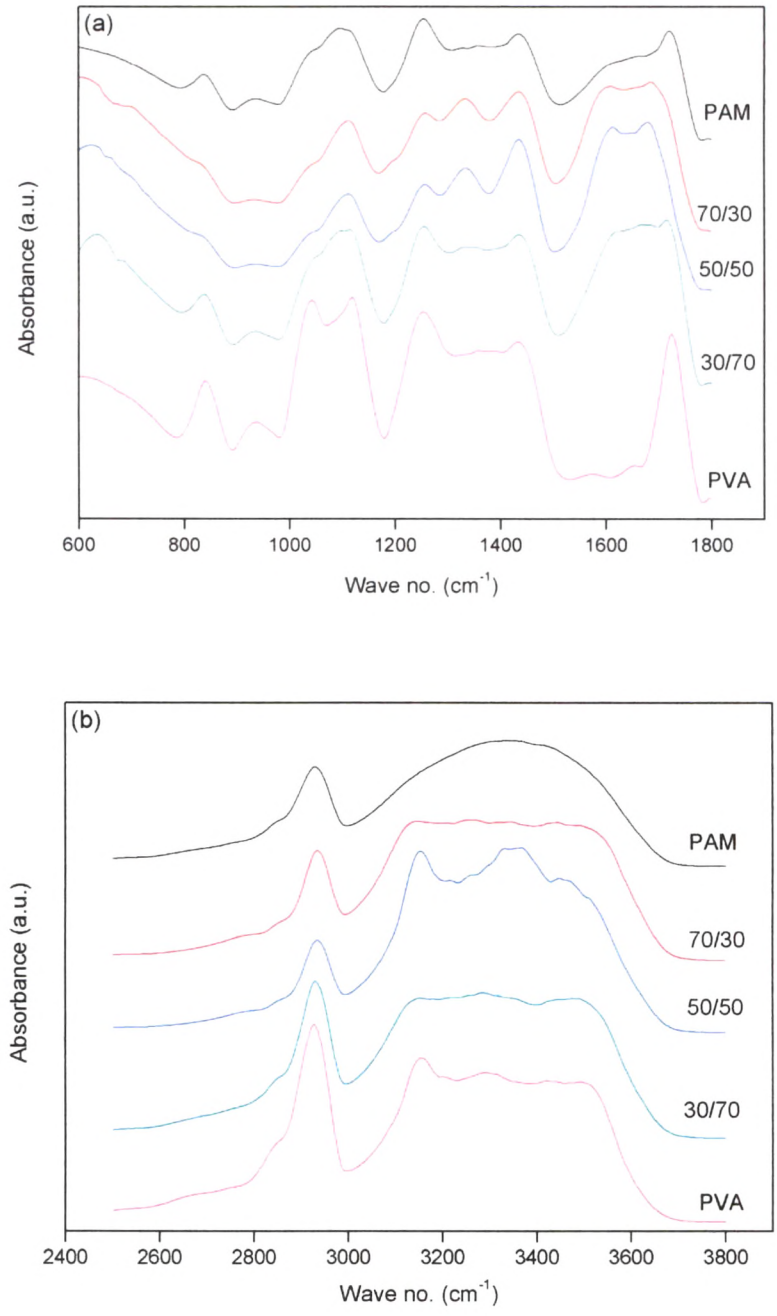

Figure 4.1 FTIR Spectra of pure PAM, pure PVA, 70/30, 50/50 and 3070 blend ratio (a) in the region of 600-1800 cm^{-1} (b) in the region of 2500-3800 cm^{-1}

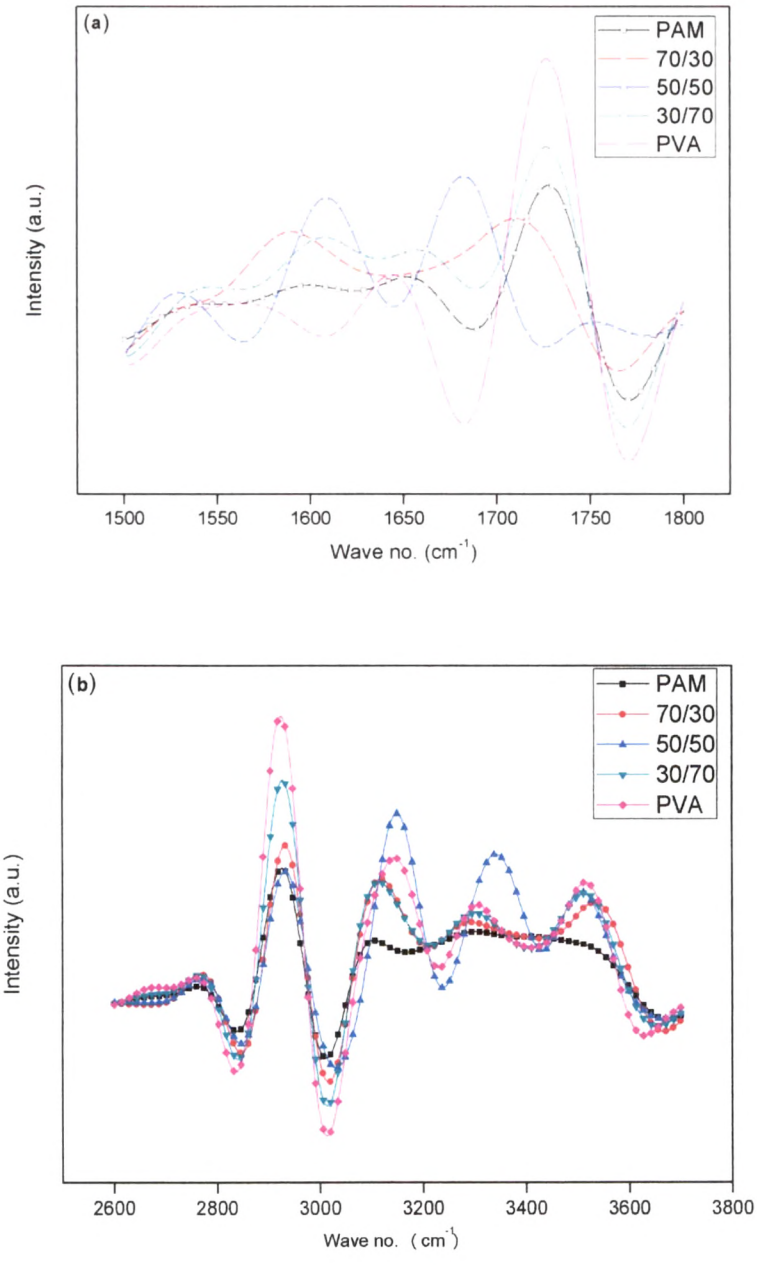

Figure 4.2 Deconvolution spectra of pure PAM, pure PVA, 70/30, 50/50 and 3070 blend ratio (a) band in the region of 1500-1800 cm^{-1} (b) band in the region of 2600-3700 cm^{-1}

Table 4.1 Assignments of the FT-IR characterization bands of the pure PAM, pure PVA and pure PAM/PVA blend[38, 39, 40]

Wave no. (cm^{-1})	Assignment (PAM)	Wave no. (cm^{-1})	Assignment (PVA)	70/30	50/50	30/70
936	C–O symmetric Stretching	936	C–O symmetric Stretching	933	934	934
1097	C–C asymmetric Stretching	1042	C–O–C symmetric Stretching	1112	1112	1115
1254	$-NH_2$ wagging	1119	C–O–C asymmetric Stretching	1258	1256	1254
1328	C–H bending	1254	$-CH_2$ bending	1334	1334	1333
1359	$-CH_2$ wagging	1360	$-CH_2$ out of plane bending	1435	1435	1435
1434	C–N stretching	1433	O–H & C–H bending	1529	1529	1547
1600	N–H bending	1565	O–H & C–H bending	1590	1608	1607
1652	Asymmetric stretching of $-COO^-$	1644	C=C stretching		1683	1658
1728	C=O stretching	1727	C=O symmetric stretching	1711	1752	1727
2763	C–H symmetric stretching	2759	$-CH_2$ symmetric stretching	2770	2770	2764
2926	C–H asymmetric stretching	2925	$-CH_2$ asymmetric stretching	2932	2933	2927
3105	N–H symmetric stretching	3145	O–H stretching	3118	3149	3114
3302	N–H asymmetric stretching	3301	O–H stretching	3291	3342	3301
		3516	O–H stretching	3534	3507	3515

Other IR bands of PAM had distinct shift as shown in the **Table 4.1**. For 50/50 there is maximum shift for different IR peaks. For 50/50, bending vibration of N-H (1600 cm^{-1}) blue shifted by 8 cm^{-1} to 1608 cm^{-1}, asymmetric stretching of –COO- (1652 cm^{-1}) blue shifted by 31 cm^{-1} to 1683 cm^{-1}, the C=O stretching vibration also blue shifted by 24 cm^{-1} from 1728 cm^{-1} to 1752 cm^{-1}. Other vibrational peaks are also blue shifted as shown in the **Table 4.1**. No shift is observed for C-N stretching vibration. Peak at 936 cm^{-1} due to CO symmetric stretching of PVA and PAM is not shifted but intensity of this peak is increased for 30/70 blend ratio while for 50/50 and 70/30 blend ratio its intensity is very negligible.

4.2.2. UV-Vis Analysis

The optical absorption (UV-Vis) spectra of pure PAM/PVA and their blends in the wavelength range 200-800 nm are shown in **Figure 4.3(a)**. From the figure pure PVA has a small weak absorption band at 272 nm. This band attributed to the $\pi \rightarrow \pi^*$ transition of C–O group of PVA [49]. Intensity of this absorption peak is slightly increased for 30/70 wt % and then almost

disappears for other blends ratio. This may be due to the increase of number of C–O group of the PVA which is also confirmed by IR spectrum that C–O stretching group intensity is maximum for 30/70 wt% while in others it almost disappears. In all the spectra we can see a sharp increase of light absorption below 220 nm which corresponds to $n \rightarrow \pi^*$ transition of amine carbonyl groups in PAM macromolecules [49]. Absorption of 50/50 wt% is maximum from all the pure and blends polymer systems in visible region. From the absorption spectra one can show that absorption edges are slightly shifted toward higher wavelength with the increase of PVA content.

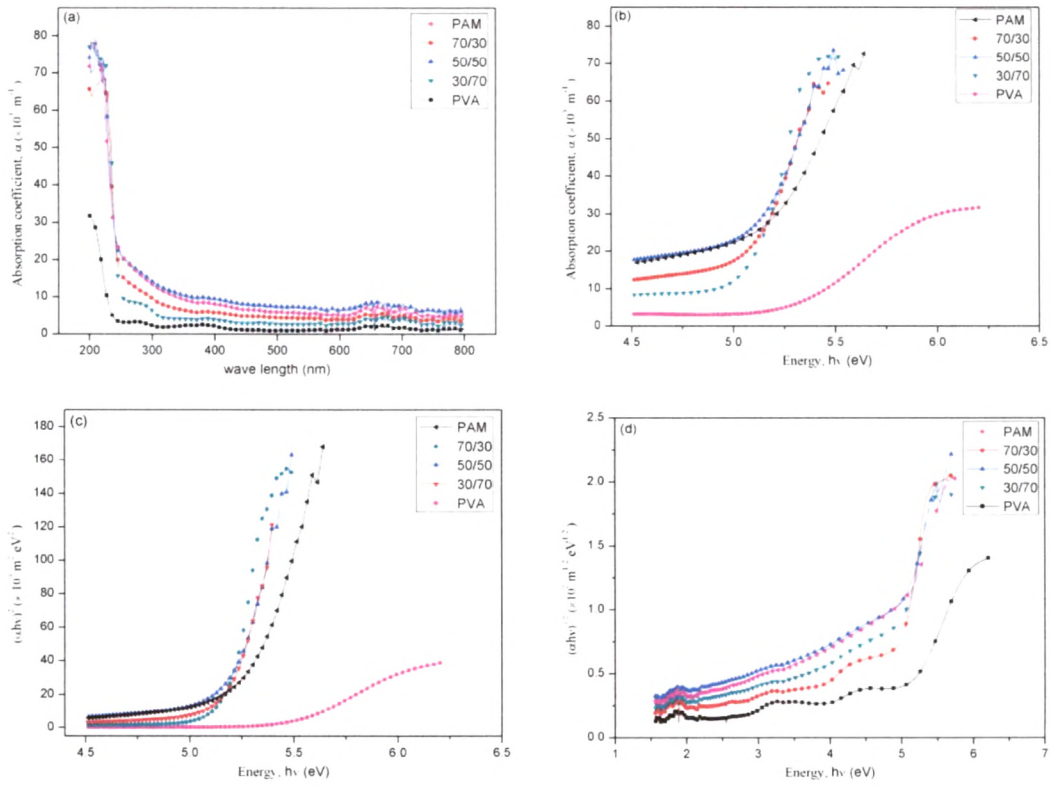

Figure 4.3 Plot of (a) Absorption coefficient (α) vs Wavelength (λ), (b) Absorption coefficient (α) vs Photon Energy (hν), (c) $(\alpha h\nu)^2$ vs hν, (d) $(\alpha h\nu)^{1/2}$ vs hν

Table 4.2 Variation of optical (Direct/Indirect) energy gap (E_g^{opt}) and absorption edge (ΔE) with different samples

PAM/PVA	Optical energy gap (E^{opt})		Absorption edge (eV)
	Direct (eV)	Indirect (eV)	
Pure PAM	5.35	4.57	4.97
70/30	5.18	4.84	5.10
50/50	5.14	4.75	4.99
30/70	5.15	4.82	5.07
Pure PVA	5.47	4.87	5.24

The absorbance process plays an important role in the optical properties of polymers. The absorption coefficient was determined from the UV-VIS spectra using the formula:

$$\alpha = A/d \quad (1)$$

Where A is the absorbance and d is the thickness of the film. The Tauc relation for dependence of absorbance on photon energy is [50].

$$\alpha(\nu) = B(h\nu - E_g)^x/h\nu \quad (2)$$

Where α (ν) is the absorption coefficient, E_g is the optical gap of the substance, h is plank's constant, ν is the corresponding frequency, x is the parameter that gives the type of electron transition. It was observed that two distinct linear relations were found for x = 1/2 (Direct transition) and x = 2 (Indirect transition), corresponding to different inter band absorption processes [51] and factor B depends on the transition probability and can be assumed to be constant within the optical frequency range [51, 52]. E_g is the optical energy gap. On the basis of equation 2, direct and indirect band gap and absorption edge were determined. The position of the absorption edge, the direct band gap and indirect band gap were obtained from the plot of α vs hν, $(\alpha h\nu)^2$ vs hν and $(\alpha h\nu)^{1/2}$ vs hν shown respectively in **Figure 4.3 (b)**, **Figure 4.3 (c)** and **Figure 4.3 (d)**. The values of the absorption edge and the direct/indirect band gap were

determined by extrapolation of the linear portions of these curves to zero absorption. The values of various optical parameters are shown in the **Table 4.2**.

Absorption edge, direct and indirect band gap were decreased as we increase PVA contents in PAM polymer matrix and they become minimum at 50/50 wt%. This may show that as a result of blending, there is the change in the number of final states in the band gap [51, 53]. And also increase in the number of defects which leads to increase in the density of localized states in the band structure which led to a decrease in the optical band gap [16].

4.2.3. RAMAN Analysis

Raman spectroscopy used for the qualitative analysis of the interaction of PVA with PAM. **Figure 4.4 (a, b)** shows FT-Raman Spectra of pure PAM, pure PVA and their blends. **Table 4.3** lists the assignments for the bands of pure polymers.

For PAM, the bands near 854 cm^{-1} corresponding to C-C stretching region of PAM. The band at 1107 cm^{-1} attributed to the C-O-C stretching modes of PAM. The band near 1400 cm^{-1} assigned mainly to the C–N stretching vibration. A band near 1711 cm^{-1} attributed to C=O stretching mode of the PAM polymer chain. In the range of the stretching vibrations of the $-CH_2$ groups, a band at 2914 cm^{-1} indicates the $-CH_2$ stretching. Two overlapped bands, around 3124 cm^{-1} and 3248 cm^{-1}, are due to $-NH_2$ symmetric and asymmetric stretching respectively.

For PVA, broad peak near 786 cm^{-1} and 988 cm^{-1} are from C-C stretching vibration and C-O-C stretching of PVA respectively. Two overlapped peak of $-CH_2$ wagging and $-CH_2$ twisting are appeared at 1333 cm^{-1} and 1398 cm^{-1} with the hump at 1577 cm^{-1} which attribute to the $-CH_2$ deformation vibration. Band appear at 2875 cm^{-1} is due to $-CH_2$ stretching while 3100 cm^{-1} and 3350 cm^{-1} are mainly due to –OH stretching of PVA. For the blends of PAM/PEO Raman band values are shown in **Table 4.4**. From the table we can see the peak shifting towards higher wave

number side. Peak shift observed for all blends, which indicates the intermolecular interaction between PAM and PVA. Maximum peak shift is observed for 50/50 wt% of PAM/PVA blend due to maximum intermolecular interaction.

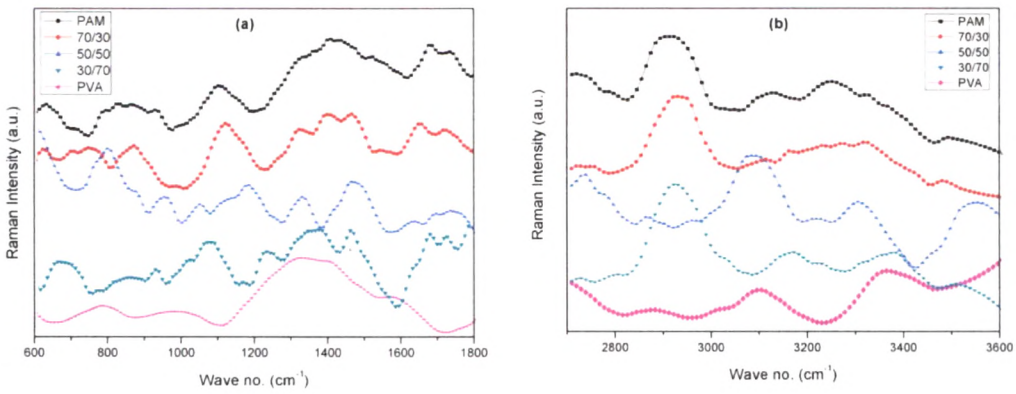

Figure 4.4 Raman Spectra of pure PAM, pure PVA, 70/30, 50/50 and 3070 blend ratio (a) in the region of 600-1800 cm^{-1} (b) in the region of 2700-3600 cm^{-1}

Table 4.3 Assignments of the Raman characterization bands of the pure PAM and pure PVA

Wave no. (cm^{-1})	Assignment (PAM)	Wave no. (cm^{-1})	Assignment (PVA)
854	C-C stretching	786	C–C Stretching
1107	C-O-C stretching	988	C–O–C Stretching
1400	C-N stretching	1333	$-CH_2$ waging
1711	C=O Stretching	1577	O–H & C–H bending
2914	$-CH_2$ stretching	2875	$-CH_2$ Stretching
3124	$-NH_2$ symmetric stretching	3145	O–H stretching
3248	$-NH_2$ asymmetric stretching	3301	O–H stretching

Table 4.4 Assignments of the Raman characterization bands of the PAM/PVA blends

Assignment	70/30	50/50	30/70
C–C Stretching	749	800	weak
C-C stretching	875	957	934
C-O-C stretching	1117	1186	1078
$-CH_2$ waging	1321	1330	1355
C-N stretching	1466	1475	1464
O–H & C–H bending, C=O Stretching	1659	1740	1680
$-CH_2$ stretching	2933	3085	2923
O–H stretching, $-NH_2$ symmetric stretching	Over Lapped	3222	3171
$-NH_2$ stretching	3271	3305	3388
O–H stretching	weak	3546	3501

For 50/50 there is maximum shift for different Raman peaks. For 50/50; Mainly stretching vibration of C-N (1400 cm^{-1}) blue shifted by 75 cm^{-1} to 1475 cm^{-1}, the C=O stretching vibration also blue shifted by 29 cm^{-1} from 1711 cm^{-1} to 1740 cm^{-1}. Other vibrational peaks are also blue shifted as shown in the **Table 4.4**.

Addition of PVA into PAM polymer matrix, bands of PAM at 3124 cm^{-1} and 3248 cm^{-1} which are symmetric and asymmetric stretching vibration of $-NH_2$ group involved in inter molecular interaction of hydrogen bond coupled with –OH group of PVA at 3145 cm^{-1} and 3301 cm^{-1}. Spectra of blends clearly indicate the increase in the intensity with well separated bands in the region of 3000 cm^{-1} to 3600 cm^{-1}. But intensity of this broad band is maximum for 50/50 blend ratio than the others and peak shifting (at 3149 cm^{-1} and 3171 cm^{-1}) in this region is toward higher wave number side, which indicates the strong hydrogen bonding between PAM and PVA due to $-CONH_2$ groups in PAM and –OH group in PVA.

4.2.4. Mechanical Analysis

Mechanical properties of PAM/PVA were carried out to study the young's modulus (Y.M.), Ultimate tensile strength (UTS), stiffness, elongation at break, stress at break, Max load taken by films as shown in **Figure 4.5(a, b)**. Mechanical properties of blends were greatly influenced by

the introduction of PVA into PAM polymer matrix, which reveals the enhanced mechanical properties such as YM, UTS, stress at break and max load. The different mechanical properties values in blends are due to the different cross linking density provided by PVA with different weight percentage of PVA [55]. Polymers have either higher crystallinity, cross linking or rigid chain exhibit a higher strength and lower extendibility that is why young's modulus and ultimate tensile strength values are higher and will give lower elongation value [55, 56].

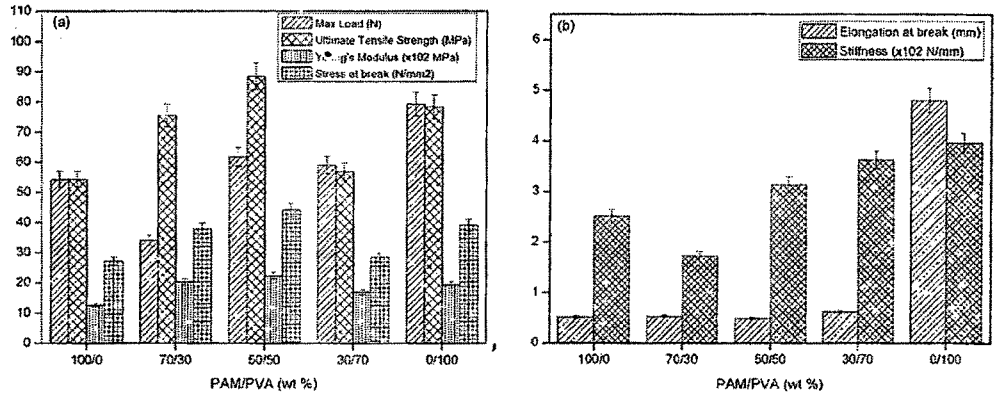

Figure 4.5 Variation in (a) Max load, Ultimate tensile strength, Young's Modulus, stress at break (b) Elongation at break, Stiffness as a function of PAM/PVA content

From the graph our results also agrees with the above conclusion. For 50/50 blend ratio the YM and UTS values are higher but elongations have lower value. Blend of PVA with PAM effectively improve the mechanical properties. When PVA is blend with PAM, interaction at molecular level occurs, which reveals the enhancement of mechanical properties. Enhancement in mechanical properties is due to the possibility of a strong hydrogen bonding between $-CONH_2$ groups in PAM and –OH group in PVA. This interaction becomes maximum for 50/50 wt% therefore we obtain maximum value of mechanical properties. This can also be correlated with IR analysis.

4.2.5. Thermal gravimetric Analysis

The thermal degradation behavior of both pure polymer PAM and PVA and their blend samples were examined by TGA as shown in **Figure 4.6 (a)**. The initial weight loss for all samples observed due to moisture evaporation. Next decomposition was major weight loss. This may correspond to structural decomposition of polymer blends and higher weight loss in this region indicates the existence of chemical degradation. The major weight losses occur in the range of 180-390 °C for all the samples. The difference in the thermal decomposition is observed clearly from derivative TG (DrTG) curve as shown in **Figure 4.6 (b)**. Other than PVA, three thermal decomposition peaks (T_p) were observed. Relevant data is shown in **Table 4.5**.

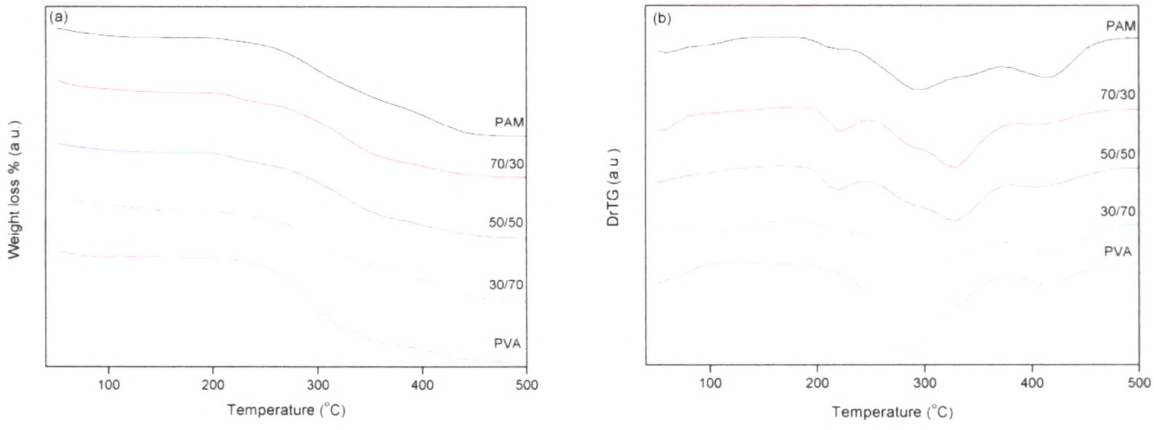

Figure 4.6 (a) TG of pure PAM, pure PVA and blends (b) Dr TG of pure PAM, pure PVA and blends

Table 4.5 TG and DrTG data of Pure PAM, PVA and their blended samples

PAM/PVA	Temperature(°C)			Weight loss (%)
	Starting	Ending	T_p	
100/0	184	220	203	8.4
	230	369	294	31.7
	377	489	415	78.1
70/30	188	246	219	13.7
	248	382	325	50.2
	391	484	407	72.9
50/50	188	241	220	12.8
	250	380	330	47.9
	382	488	405	69.2
30/70	185	221	209	10.9
	228	368	295	32.2
	375	484	400	67
0/100	175	380	290	40.2
	382	475	416	86.2

T_p (Peak Temperature) of DrTG is a function of blend weight percentage. T_p was used as a measure of thermal stability. Thermal stability of blend is higher than the pure PAM, as indicated by the shift in T_p towards higher temperature. T_p was maximum for 50/50 wt %, so this blend is more stable. This higher thermal stability was observed for 50/50 blend sample by TGA and DrTG were due to the intermolecular crosslinking reaction which gave highly compatible impact blend system [16, 54]. From the data obtained by TGA indicates the possibility of a strong hydrogen bonding between PAM and PVA due to $-CONH_2$ groups in PAM and –OH group in PVA, which is also confirmed by our FTIR study.

From TGA, we conclude that the thermal stability regions of the blend samples were higher than the PAM and stability enhanced by increasing PVA content in PAM polymer matrix and it become more stable for 50/50 wt%.

4.2.6. Scanning Electron Microscopy

From SEM image for PAM and PVA (**Figure 4.7(a), (b)**), smooth and homogeneous surface with some straps obtained. Formation of homogeneous blends was mostly caused by the interaction of hydrogen bonds between functional groups of blend components [57].

As shown **Figure 4.8 (a), (b)** and **(c)**, blends surfaces have heterogeneous mesh type morphology. This is possibly due to PVA, linear polymer, cross linked with PAM may form clusters/domains of chains bonding via hydrogen bond between $-CONH_2$ groups in PAM and –OH group in PVA. At low content of PVA, crosslinking density is low. So the network chains have good movement and arrange themselves to make mess type of domain network. As PVA content increase, mesh/domain size goes on shrinking. A change in morphology toward smaller domains of a dispersed PVA is expected to give rise to an improvement in the mechanical properties. From SEM micrograph, interaction between PAM and PVA is much greater than others and surface of 50/50 blend ratio is rougher than the other blends. SEM analysis also indicates enhancement in thermal and mechanical properties.

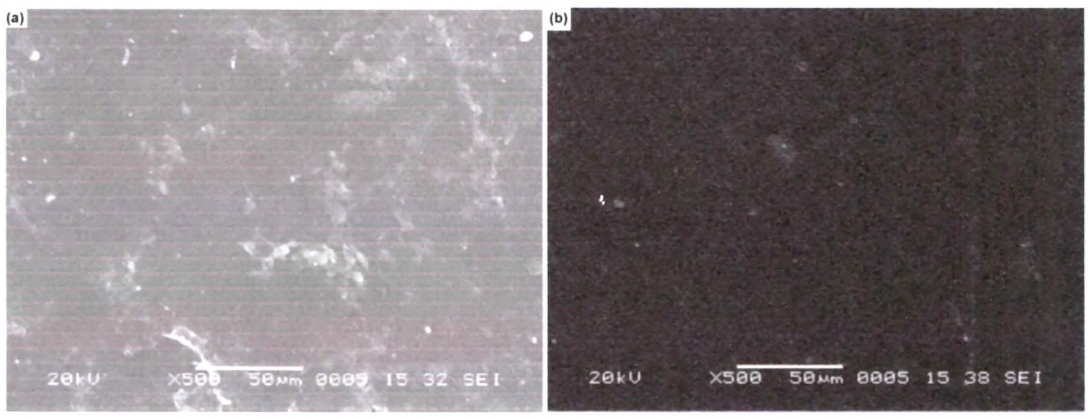

Figure 4.7 Scanning Electron Micrograph of (a) Pure PAM (b) Pure PVA

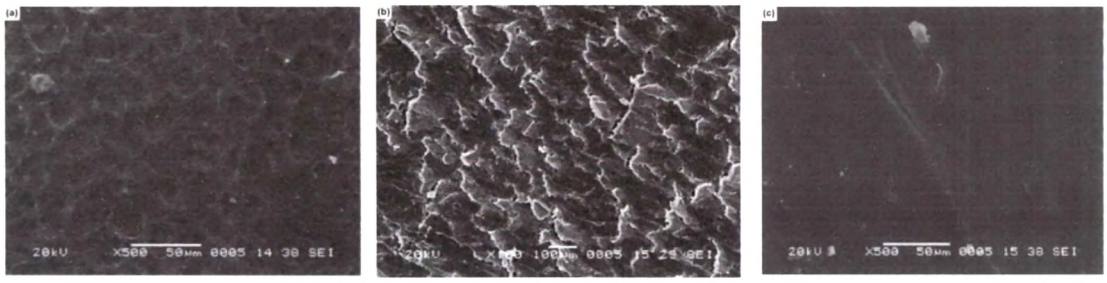

Figure 4.8 Scanning Electron Micrograph of (a) 70/30 (b) 50/50 (c) 30/70

4.3. Conclusions

FTIR and Raman analysis confirmed the conclusion about the specific hydrogen bonding interaction between –CONH2 groups in PAM and –OH group in PVA. The maximum blue shift of IR peaks of 50/50 wt% implies that bond strength is increased. And that's why; thermal stability and mechanical properties are increased maximum for 50/50 wt%. So we directly correlate enhancement of thermal stability and mechanical properties by noticing the blue shift of IR peak which are contributed to intermolecular interaction between polymers. From UV-Vis studies, noticeable changes in absorption spectra were observed and change in various optical parameters also confirmed that intermolecular interaction occur between PAM and PVA. The position of absorption edge was slightly shifted towards higher wavelength side. Morphological changes in the blend samples were also explained and result was also correlated with the other studies. So from this study we concluded that blend of PAM/PVA with 50/50 wt% is most suitable and compatible with most enhancing properties.

4.4. References

1. Tuncer CA, Serkan D. Journal of Macromolecular Science, Part A: Pure and Applied Chemistry 43:1113–1121, 2006.
2. Lopatin VV, Askadskii AA, Peregudov AS, Vasilev VG, J. Appl. Polym. Sci. 96:1043–1058. 2005.
3. Durmaz S, Okay O, Polym. Bull. 46:409–418, 2001.
4. El-Sabbagh S, Mokhtar SM, Messieh SLA, Journal of Applied Polymer Science 70:2053–2059, 1998.
5. Ratner BD, Hoffman AS, Schoen JF, Lemons JE. Biomaterials Science, an Introduction to Materials in Medicine. Academic Press, New York, 1996.
6. Bajpai AK, Bhanu S, J. Mater. Sci. Mater. Med. 15:43-54, 2004.
7. Peppas NA, Langer R, New challenges in biomaterials. Science 263:1715-1720, 1994.
8. Aalaie J, Farahani EV, Iranian Polymer Journal 21(3):175-183, 2012.
9. Abdelhak M , Abdelkarim H, Barbara I, J. Chem. Chem. Eng. 6:7-17, 2012
10. Lee KE, Poh BT, Morad N, Teng, Int. J. Polym. Anal. Charact. 13:95-107, 2008.
11. Lee KE, Poh BT, Morad N, Teng TT, J. Macromol. Sci. A 46:240-249, 2009.
12. Rho T, Park J, Kim C, Yoon HK, Suh HK, Polym. Degrad. Stab. 51:287-293, 1996.
13. Yang MH, Polym. Degrad. Stab. 76:69-77, 2002.
14. Wallace A, Wallace GA, Abouzam AM, Soil Sci. 141:377-380, 1986.
15. Rosen J, Hellenas KE, Analyst 127:880-882, 2002
16. El-Kader FH, Gafer SA, Basha AF, Bannan SI, Basha MAF, Journal of Applied Polymer Science 118:413–420, 2010.

17. Cholakis C H, Zingg W, Sefton M V, J Biomed Mater Res. 23:417-441, 1989.

18. Horiike S, Matsuzawa S, J. Appl. Polym. Sci. 58:1335-1340, 1995.

19. Vargas R A, Garcia A, Vargas M A, 43:1271-1274, 1998.

20. Fritz H P, Breitsmer M, Solid State Ionics 45:255-260, 1991.

21. Peppas N A Hydrogels in Medicine and Pharmacy. Polymers, CRC Press, Boca Raton, vol. II, 1987.

22. Rajendran S, Mahendran O, Ionics 7:463-468, 2001.

23. Coleman M M, Painter P C, Prog. Polym Sci. 20:1-59, 1995.

24. Jahanshahi M, Rahimpour A, Mortazavian N, Iranian Polymer Journal 21(6):375-383, 2012.

25. Yeom CK, Lee KH, J. Membr. Sci. 109:257- 265, 1996.

26. Muhlebach A, Muller B, Pharira C, Hofmann M, Seiferling B, Guerry DJ, Polym. Sci. Part A: Polym. Chem. 35:3603-3611, 1997.

27. Kim KJ, Lee SB, Han NW, Polym J. 25:1295-1302, 1993.

28. Rafienia M, Zarinmehr B, Poursamar SA, Bonakdar S, Ghavami M, Janmaleki M, Iranian Polymer Journal 22(2):75-83, 2013.

29. Tanga Q, Huanga K, Qianb G, Brian C, Benicewicz, Journal of Power Sources 229:36-41, 2013.

30. Zhang X, Burgar I, Lourbakos E, Beh H, Polymer 45:330S–3312, 2004.

31. El-din HMN, El-Naggar AWM, Faten IA, Polym Int. 52:225–234, 2003.

32. Xu N, Zhou D, Li L, He J, Chen W, Wan F, Xue G, J Appl Polym Sci. 88:79–87, 2003.

33. Barretta P, Bordi F, Rinaldi C, Paradossi G, J Phys Chem B 104(47):11019–11026, 2000.

34. Chan LW, Hao JS, Heng PWS, Chem Pharm Bull. 47(10):1412–1416, 1999.

35. Hassan CM, Peppas NA, Adv Polym Sci. 153:37–65, 2000.

36. Russo R, Macinconico M, Petti L, Romano G, J Polym Sci Part B: Polym Phys. 43(10):1205–1213, 2005.

37. Elashmawi IS, Hakeem NA, Abdelrazek EM, Physica B 403:3547– 3552, 2008.

38. Mohan S, Murugan R, Arabian J Sci Eng. Sect. A 22(2A):155–164, 1997.

39. Murugan R, Mohan S, Bigotto A, J Korean Phys Soc. 32(4):505–512, 1998.

40. Deng Y, Dixon JB, White GN, Loeppert RH, Anthony S, Juom R, Colloids and Surfaces A: Physicochem Eng Aspects 281:82–91, 2006.

41. Freddi G, Tsukada M, Beretta S, J Appl Polym Sci. 71:1563-1571, 1991.

42. Yan F, Zheng CR, Zhai XD, Zhao DJ, J Appl Polym Sci. 67:747-754, 1998.

43. Li X, Goh SH, Lai YH, Wee ATA, Polymer 41:6563-6571, 2000.

44. Abdelaziz M, Abdelrazek EM, Physica B 390:1-9; 2007.

45. Laot CM, Marand E, Oyama HT, Polymer 40:1095-1108, 1999.

46. Abdelrazek EM, Elashmawi IS, Labeeb S, Physica B 405:2021–2027, 2010.

47. Knudsen R, Sala O, Hase Y, J. Mol. Struct. 321(3):197-203, 1994.

48. Raaska T, Kunttu H, Räsänen M, Luppi J, Pajunen P, J. Mol. Struct. 221:195-208, 1990.

49. Patel G, Sureshkumar MB, Patel P, AIP Conf. proc. 1349:166-167, 2011.

50. Tauc J, Grigorovici R, Vanku A, Phys. Stat. Sol. (b) 15:627-637, 1966.

51. Shahada L, Kassem ME, Abdelkader HI, Hassan HM, J. Appl. Polym. Sci. 65:1653-1657, 1997.

52. Mott N F, Davis E A, Electronic processes in Non Crystalline materials. 2nd edn. Oxford university press, Oxford, 1973.

53. El-Samanoudy M M, Ammar A H, Status Solidi A 187(2):611-621, 2001.

54. Aggour YA, Polm. Degrade. Stab. 51:265-269, 1996.

55. Patel G, Sureshkumar MB, Singh NL, Bhattacharya SS, Journal of International Academy of Physical Sciences 14:91-100, 2010.

56. Chi SK, Seung MO, Electrochim acta 46:1323-1331, 2001.

57. Chen CH, Wang FY, Mao CF, Liao WT, Hsieh CD, International Journal of Biological Macromolecules 43(1):37-42, 2008.